This article has been accepted for inclusion in a future issue of this journal. Content is final as presented, with the exception of pagination.

The Applicability of Dual Stage Ion Optics to Ion Engines for High Power Missions

Michele Coletti and Stephen B. Gabriel

***Abstract*—In this paper, the applicability of dual stage ion optics and in particular of the so-called dual stage ion engine to high power, high specific impulse missions will be evaluated. First, the performance limits of conventional two gridded ion engines (GIE) will be discussed and the advantages provided by dual stage ion engines reported. The limits of applicability of a dual stage ion engine will be analyzed analytically and the results confirmed numerically. The lifetime and performance of a three gridded dual stage ion engine (DS3G) will be numerically investigated and compared to those of a conventional GIE assessing for the first time in the open literature under what condition dual stage ion optics provide performance improvements over conventional GIEs and what is its impact on the thruster lifetime. Dual stage ion engines have been found to be capable of providing higher thrust density and longer lifetime with respect to conventional gridded ion engines.**

***Index Terms*—Dual stage ion engine, gridded ion engine, HiPER, ion opics, space propulsion.**

NOMENCLATURE

A_g	grid area
d	grid separation
E	electric field
f	focal length
g_0	gravitational acceleration at sea level
I_{beam}	ion beam current
Isp	specific impulse
J_i	ion current density
l_e	effective distance between the first and second grid
m_i	ion mass
P	perveance
P_{max}	perveance at the Child-Langmuir limit
q	electron charge
r	grid aperture radius
t	grid thickness
T	thrust
T_g	grid transparency
V	grid potential
V_{min}	minimum centerline potential at the accel grid
Δv	velocity change required to complete a mission
ΔV_{sc}	space charge contribution to V_{min}
ΔV_{geom}	geometric contribution to V_{min}
ε_0	vacuum dielectric constant
λ	grid spacing ratio
θ	ion beam divergence angle
Γ	acceleration to extraction voltage ratio
Subscript	
1	relative to the first grid
2	relative to the second grid
3	relative to the third grid
a	relative to the accel grid

Manuscript received July 11, 2011; revised October 25, 2011 and January 20, 2012; accepted January 20, 2012. This work was supported by European Community's Seventh Framework Programme ([FP7/2007-2013]) under Grant agreement no 218859.

M. Coletti is with the Astronautics Research Group, University of Southampton, SO17 1BJ Southampton, U.K. (e-mail: coletti@ soton.ac.uk).

S. B. Gabriel is with the University of Southampton, SO17 1DR Southampton, U.K. (e-mail: sbg2@soton.ac.uk).

Color versions of one or more of the figures in this paper are available online at http://ieeexplore.ieee.org.

Digital Object Identifier 10.1109/TPS.2012.2185953

I. INTRODUCTION

RECENTLY, both the USA and Europe have studied and launched (or are about to launch) ambitious space missions like Dawn [1]–[3], Deep Space 1 [4], GOCE [5] and Bepi Colombo [6]. These missions are so demanding in terms of the required velocity change (Δv) and lifetime that they can be accomplished only with the use of electric propulsion and, in particular, using an electric propulsion technology that provides high Isp and long operational lifetime. The kind of thrusters that best suit these requirements are gridded ion engines (GIE) due to their high total efficiency (50–70%), high specific impulse (of the order of 3500 s for commercial devices and more for science missions thrusters), and long lifetime (tens of thousands of hours).

The working principles of a GIE rely on the ionization of a large fraction of an inert propellant (commonly Xenon) and in the acceleration of these ions with the use of a set of grids biased to different voltage levels; their power inputs range from fractions of a kW to several kW, thrust levels from 0.002 to 0.7 N, and specific impulses ranging from 2500 to 9000 s.Their main limitation is the maximum thrust that can be produced per grid unit area (thrust density) due to the fact that the extraction of the ions and their acceleration processes are deeply interconnected [7]. Considering that engineering limits exist to the maximum grid size (mainly due to structural resistance to the launch mechanical loads) [8], the GIE limit on thrust density poses an upper limit on the maximum thrust achievable with such devices and, consequently, on the maximum power that a single GIE can process.

0093-3813/$31.00 © 2012 IEEE

This article has been accepted for inclusion in a future issue of this journal. Content is final as presented, with the exception of pagination.

At present, ambitious high-power missions like building infrastructures on the L1 point of the Earth Moon system, exploration of outer planet of the solar system, and building of infrastructures on Mars are under study in Europe under the HiPER project [9]. In this paper, we will use the requirements of these missions as a starting point for the discussion of the applicability and performance of dual stage ion optics; nevertheless, the results so obtained are of a much wider nature and applicable to any high power mission requiring high specific impulse.

GIEs have already been successfully used for very challenging missions like Dawn [1]–[3], Hayabusa [10], Deep Space 1 [11], GOCE [12] and will be used for Bepi Colombo [13]; hence, they have been included as a candidate technology for application to future high power, high specific impulse missions like the building of infrastructures on the EML1 point and on Mars. Nevertheless, considering that these missions will baseline a power per thruster of 25–50 kW and the use of clusters made up of several thruster (up to 8) [9], the limitation in thrust density of GIEs will pose concerns to their applicability due to the mechanical resistance of the grids and the total area required to accommodate the thrusters.

A solution to overcome the thrust density limitation of GIE was envisaged by D. Fearn with the application of multistage acceleration to ion engines [14]. Multistage ion acceleration is a concept commonly used in the field of fusion research to inject high energy particles in tokamaks where a set of multi-aperture grids is used to extract ions from a plasma and accelerate them up to MeV energy level [15]–[20].

This new kind of thruster was named dual stage four gridded ion engine (DS4G) and a technology demonstrator was built and tested by ESA-ESTEC in collaboration with Fearn and the Australian National University demonstrating the possibility of using multistage ion optics on a space thruster [14], [21]. During these tests, no attempts were made at the optimization of the ion optics, and, because of the high voltages involved and limited resources, several experimental difficulties with insulation, reliability, and direct ion impingement were encountered [22].

At present, the limits of applicability of a dual stage ion engine in terms of the operating conditions at which its use will be beneficial in terms of thrust density in comparison to a conventional GIE are still unexplored. Even more importantly, unexplored is the effect that the use of multistage acceleration will have on the thruster lifetime. Moreover, for what concerns lifetime, no data can be extrapolated from multistage particle acceleration devices used in fusion research since their functioning is normally limited to short periods of time not comparable with the tens of thousands of hours of operating lifetime that are commonly required by ion engines.

In this paper, these two questions will addressed by studying the limits of applicability of a dual stage ion engine, numerically investigating the lifetime of such a thruster, and comparing the results so obtained to the requirements of Deep Space 1, Dawn, GOCE, Bepi Colombo and of futuristic high power mission like the building of infrastructures on the Earth Moon L1 point and on Mars and a NEP mission to Saturn.

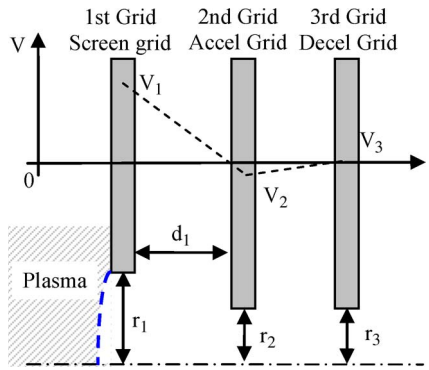

Fig. 1. Conventional GIE ion optics schematic.

II. Conventional Gridded Ion Engines

Existing GIEs conventionally use two grids. The first grid (screen grid) is held at high positive potential (normally around 750–2000 V), the second grid (accel grid) is at negative potential (about -200 V) and has the double function of providing the needed potential drop to extract and accelerate the ions and to prevent the backstreaming of electrons from the plasma formed downstream of the thruster back into the discharge chamber. If a third grid is present (decel grid), it is normally held at a potential close to the beam plasma potential and has the sole function of protecting the accel grid from the impact of the charge exchange ions (CEX) created in the downstream plasma that tend to backstream toward the accel grid due to its negative voltage. The benefits obtained from the use of a decel grid are normally outweighed by the increase in complexity relative to its presence, and, for this reason, it is commonly not used [7].

A. Performance of Conventional GIEs

To understand the ion extraction process and how this influences the performance and lifetime of a GIE, we will refer to the perveance of the extraction system (P)[23], [24]

$$P = \frac{I}{\Delta V^{3/2}} \tag{1}$$

where I is the extracted current and ΔV the extraction voltage drop $(\Delta V = V_1 - V_2)$. The perveance is strongly linked to the space charge effects relative to the extraction of an ion current and its maximum value can be obtained using the Child-Langmuir equation [7] as

$$P_{\max} = \frac{4\pi\varepsilon_0}{9}\sqrt{\frac{2q}{m_i}}\frac{r_1^2}{d_1^2} \tag{2}$$

where P_{max} is the perveance at the Child Lagmuir limit, ε_0, q and m_i are, respectively, the vacuum dielectric constant, the electron charge, and the mass of the extracted ions, r_1 is the first grid aperture radius, and d_1 the separation between the first two grids (Fig. 1). From the knowledge of the grid voltages and of their spacing and assuming to be in space charge limited

This article has been accepted for inclusion in a future issue of this journal. Content is final as presented, with the exception of pagination.

conditions, the performances of a GIE in terms of extracted current and specific impulse can be derived as [23]

$$J_i = \frac{4\varepsilon_0}{9}\sqrt{\frac{2q}{m_i}}\frac{(V_1-V_2)^{3/2}}{d_1^2} = \frac{4\varepsilon_0}{9}\sqrt{\frac{2q}{m_i}}E^2\sqrt{\frac{1}{V_1-V_2}} \quad (3)$$

$$Isp = \frac{1}{g_0}\sqrt{\frac{2qV_1}{m_i}} \quad (4)$$

where $E = (V_1 - V_2)/d_1$ is the electric field in between the two grids, V_1 and V_2 are, respectively, the voltages on the first and second grid relative to the spacecraft ground (Fig. 1), and d_1 is the separation between the first two grids. From (3) and (4), the thrust density can be derived as

$$\frac{T}{A_g} = J_i(g_0 Isp)\frac{A_{open}}{A_g} = \frac{8\varepsilon_0}{9}E^2 T_g \cos\theta\sqrt{\frac{V_1}{V_1-V_2}} \quad (5)$$

where A_{open} and A_g are, respectively, the grid open and total area, $T_g = A_{open}/A_g$ and T is the thrust.

According to (3) and (5), the extracted current density and the thrust density can be augmented by increasing the electric field between the grids or by reducing the potential difference keeping the electric field constant.

The variations of both these parameters are limited since an increase of the electric field in the first gap over a threshold level will cause arcing between the grids, and since the value of V_1 is fixed by the desired specific impulse and V_2 by the occurrence of electron backstreaming.

In fact, if the voltage of the second grid is not chosen carefully, the electrons present in plasma formed by the neutralized ion beam downstream of the thruster will have enough energy to backstream into the ion optics and eventually into the discharge chamber. Such flow of electrons will cause large thrust losses drastically affecting the thruster efficiency and may also lead to overheating of internal components leading to the impossibility of operating the GIE. For this reason, a negative voltage is always applied to the second grid, and, given the electron and ions densities and temperatures commonly found in the downstream plasma of GIEs, voltages less negative than -100 V cannot be commonly employed [25].

Another limitation to the achievable current and thrust density is relative to the extraction process itself and on the effect that this has on the thruster lifetime. In fact, if the working perveance of the grids exceeds the P_{max} value, the sheath existing between the discharge chamber plasma and the ion optics will start to protrude inside the ion optics region [26] producing ion trajectories that directly impinge on the second grid seriously compromising the thruster performances and lifetime. Considering that the second grid holes are normally smaller than the first grid ones to retain the non-ionized propellant, working perveances no higher than 50% of P_{max} are conventionally used [7].

From these considerations, it is clear how the thrust density produced by a conventional GIE is limited by the maximum electric field that can be applied between the grids. In particular, assuming that the electric field is kept constant, the thrust density is almost independent of the value of V_1, and hence from the chosen Isp since, according to (3)–(5), an increase in V_1 (and hence in Isp) will produce an equivalent decrease in the extracted current density. The assumption according to which the electric field is kept constant can be justified noting the fact that in existing GIEs, the electric field between the grids is commonly maximized to achieve high performance while at the same time avoiding arcing, hence any significant increase in Isp (V_1) will have to be balanced by an increase in the stage gap keeping the electric field constant.

TABLE I
MAIN PERFORMANCE PARAMETERS FOR SOME HIGH-POWER ION THRUSTERS

Thruster	Power [kW]	Thrust [N]	Grid Active area[a] [cm^2]	Thrust Density [N/m^2]	Specific Impulse [s]
HiPEP [27]	39.3	0.670	3730	1.8	9620
NEXIS [28]	23.2	0.475	2550	1.9	7500
NEXT [29]	6.9	0.237	1020	2.3	4180
XIPS [7]	4.3	0.166	490	3.4	3550
NSTAR [7]	2.3	0.093	640	1.5	3130
JAXA [30]	4.6	0.210	960	2.2	3500
RIT XT [31]	8.1	0.218	350	6.2	6420
T6 [32]	4.5	0.145	380	3.7	4120

[a] All the thrusters in the table have circular grids apart from HiPEP that has rectangular grids

TABLE II
REQUIREMENTS OF SOME HIGH POWER, HIGH SPECIFIC IMPULSE MISSIONS [9]

Mission Class	Thruster Power Class [kW]	Specific Impulse [s]	Thrust [N]
Infra-structure to Earth-Moon L1	25	5000	0.82
		10000	0.4
NEP missions to Saturn	25	10000	0.4
		15000	0.31
Mars Infra-structure	50	10000	0.66

III. REQUIREMENTS FOR FUTURE HIGH POWER SPACE MISSIONS

In Tables I and II, the performance of some existing high power GIE and the requirements for some of the HiPER missions are reported.

Comparing the data in Tables I and II, it can be noted how only two of the existing thrusters (NEXIS and HiPEP) are able to meet some of the thrust requirements and, in the case of HiPEP, providing an Isp close to the one needed by the high power missions reported in Table II. Regarding the other thrusters, they are either not able to meet any of the requirements or, in the case of the RIT thruster, they are able to provide an Isp well in excess of 5000 s but delivering a thrust that is only one quarter of the required one.

This article has been accepted for inclusion in a future issue of this journal. Content is final as presented, with the exception of pagination.

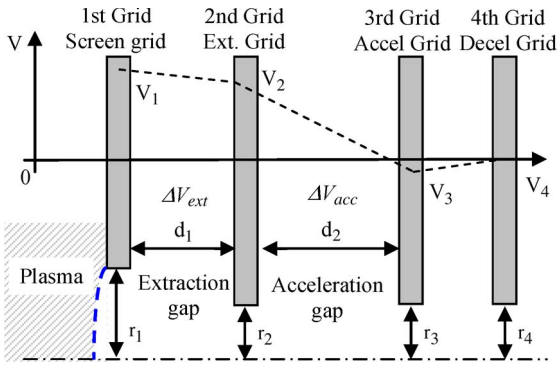

Fig. 2. Voltage profile through the grids of a four grid dual stage GIE.

If we now concentrate on NEXIS and HiPEP (since the other thrusters will need to be heavily modified to meet the HiPER requirements), and we consider that a cluster of either 6 or 8 thrusters is to be used, a total grid area of either 2.2 to 3 m^2 for HiPEP and of 1.5 to 2 m^2 for NEXIS will be needed. Such a large grid area would be clearly unpractical; hence, the need of increasing the thrust density produced by GIEs to meet the HiPER requirements with an electric propulsion subsystem of acceptable dimensions.

IV. Dual Stage Ion Optics

From (3)–(5), it can be seen that, in a conventional GIE, assuming that the electric field is kept constant, an increase in Isp leads to an almost equivalent decrease in the extracted current density hence producing a very limited increase in thrust density. The difficulties in increasing the thrust density due to the interdependence between Isp and extracted current can be overcome by using dual stage acceleration.

In a dual stage ion optics system, three or four grids are employed (Fig. 2). The first grid (screen grid) as in single stage ion optics is kept at high positive potential, the second grid (extraction grid) is kept at a positive potential lower than the first grid and has the only function of providing the potential difference needed to extract the desired current, the third grid (accel grid) is kept at negative potential and has the dual function of providing the potential difference to accelerate the ions and to repel the downstream electrons avoiding backstreaming, the fourth grid (decel grid), if present, has the function of protecting the accel grid from the impact of CEX ions created in the downstream plasma.

In such a setup, the extraction and acceleration processes of ions take place in different areas and are hence not as deeply interconnected as they are in single stage devices. Equations (3)–(5) stay formally the same for a dual stage ion optics system with the only difference that now the value of V_2 can be changed freely, and hence the extracted current and Isp are no longer formally interconnected. This allows increasing the thrust density by keeping a constant extracted current and increasing specific impulse. The limit in such increase lies in the ability of designing a second stage able to accelerate the ions avoiding direct impingement.

However, before the use of dual stage acceleration for an ion engine can be considered to be a viable and useful option, two fundamental questions need to be answered:

1) under what conditions is the increase in performance large enough to justify the increase in system complexity?
2) what impact will the use of dual stage acceleration and the consequent use of high potentials have on lifetime?

Both questions will be answered for the first time in this paper, respectively, in Sections V and VI

V. Limits of Applicability of Dual Stage Ion Optics on GIE

In this section, the limits of applicability of dual stage ion optics on GIEs in terms of the operating conditions for which the increase in performance will be enough to justify the increase in system complexity will be investigated.

As it has been said above, in a dual stage ion optics system, the extraction and acceleration processes are decoupled, hence it might be inferred that the selection of the extracted current and accelerating potential drop (hence specific impulse) are completely independent. In reality, in an ion engine, it is desirable to have a well collimated ion beam. There are two justifications for this: the first one is that, as it can be seen in (4) and (5), the beam divergence has a negative effect on the thruster performance in terms of Isp and thrust; the second one is relative to interference with the spacecraft since the wider the plume the greater the need for careful consideration of the location of the thruster with respect to other spacecraft surfaces.

If a collimated beam is desired, an extra constraint is imposed on the system causing the entity of the acceleration process to influence the ion extraction in terms of the optimum perveance ratio P/P_{max} needed to produce an (ideally) zero-divergence ion beam. This effect can be easily understood by representing each of the grids as electrical lenses of focal length f equal to [33]

$$f = \frac{4V}{E_{down} - E_{up}} \tag{6}$$

where V is the beam energy in eV at the grid aperture and E_{up} and E_{down} are the electric fields upstream and downstream of the grid. Using (6), a dual stage ion optics (where the decel grid has been omitted) can be represented as shown in Fig. 3.

As it can be seen in Fig. 3 the lens corresponding to the second grid is either convergent or divergent depending on the relative strength of the electric field in the first and second gap. When the field is weaker in the first gap than in the second ($E_1 < E_2$), the lens is converging, hence a flatter shape of the plasma sheath (and consequently a higher perveance ratio) is required to obtain a collimated jet, whereas if the contrary happens ($E_1 > E_2$), the plasma sheath needs to penetrate more into the plasma to produce more converging ion trajectories to compensate the presence of two diverging lens; this causes a reduction of perveance and hence a reduction of the total extracted current [34].

This change in optimal perveance can be studied as a function of the ratio of the potential drop applied to the acceleration

This article has been accepted for inclusion in a future issue of this journal. Content is final as presented, with the exception of pagination.

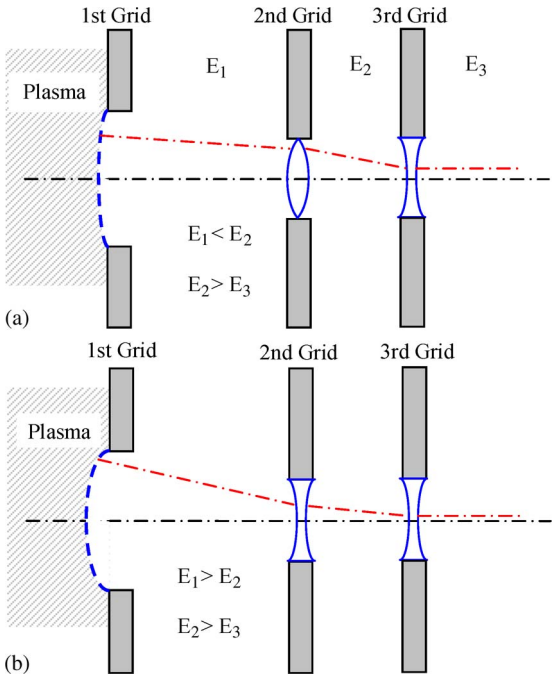

Fig. 3. Sketch of a dual stage ion engine extraction system using the electric lens analogy for (a) $E_1 < E_2$ and (b) $E_1 > E_2$.

stage to the one applied in the extraction stage. To do so, the analytical model developed by Kim, Whealton, and Schilling [34] will be used. According to this model, the beam divergence can be expressed as

$$\theta_{DSGIE} = 0.62S\left[\frac{P}{P_{\max}} - 0.4\frac{r_2}{r_1}\frac{\Gamma^2}{\lambda(1+\Gamma)} + 0.53\frac{r_2}{r_1} - 1\right] + 0.31S\left(\frac{P}{P_{\max}}\right)\left[1+\frac{t_2}{t_1} + 0.35\frac{r_2}{r_1}\left(\lambda + \frac{t_3+t_2}{d_1}\right) \times (1+0.5\Gamma)^{-1.5}\right] \quad (7)$$

where P is the working perveance, r and t stand, respectively, for the grids aperture radii and thicknesses (Fig. 2), $\lambda = d_2/d_1$ is the ratio between the first and second stage grid gaps, $S = r_1/d_1$ is the first grid hole aspect ratio, and $\Gamma = (V_2 - V_3)/(V_1 - V_2)$ is the ratio between the acceleration and extraction potential drops. In particular, it must be noted how for a fixed extraction voltage, an increase in Γ corresponds to an increase in Isp (since the higher Γ, the higher the acceleration voltage drop and hence the total voltage drop $\Delta V_{tot} = \Delta V_{acc} + \Delta V_{ext}$), whereas for a fixed Isp, an increase in Γ corresponds to a decrease in the extraction voltage.

Assuming a grid geometry and imposing $\theta_{DSGIE} = 0$, the perveance ratio P/P_{max} needed to produce a zero divergence jet can be calculated using (7). The same can be done for a conventional GIE as shown by Coupland [35]

$$\theta_{GIE} = 0.29S\left(1 - 2.14\frac{P}{P_{\max}}\right). \quad (8)$$

Fixing the ratios r_2/r_1 and t_2/t_1 using values commonly found in typical GIEs ($r_2/r_1 = 0.8$ and $t_2/t_1 = 4$), the values

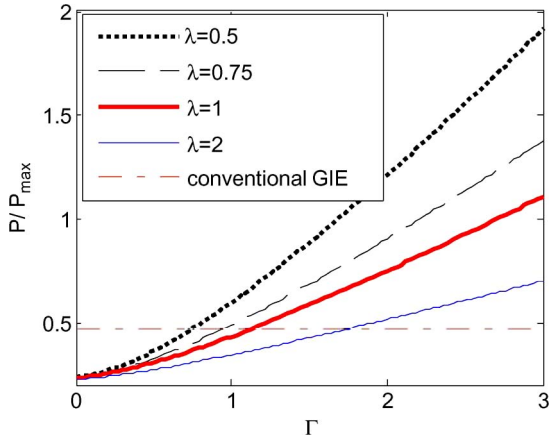

Fig. 4. Optimal $P/P_{\max}$ value for different values of Γ and λ.

of P/P_{max} needed to obtain a zero divergence jet according to (7) and (8) are shown in Fig. 4.

Looking at Fig. 4, it can be seen how for a dual stage ion optics a reduction in Γ produces a reduction in the optimum value of perveance needed to produce a zero-divergence beam. Assuming a constant extraction voltage this means that the lower the Isp, the lower the optimum working perveance and hence the extracted current. In particular, the optimum value of P/P_{max} for a dual stage ion engine falls below the one of a conventional GIE for values of Γ lower than 0.7–1.5 depending on λ. This reduction in the working perveance could be balanced moving toward lower values of the ratio between the grid spacing in the second and first stage (λ). Reducing the value of λ means either increasing the first stage gap (but this, according to (2), will cause a decrease in P_{max}) or decreasing the grids spacing in the acceleration stage. However, it must be noted that the minimum value of grid spacing is limited by the maximum electric field that can be applied between two grids before arcing happens and by structural and engineering limits, i.e., the grids and their supports need to be physically machinable, assemblable, and able to sustain thermal loads during operation and vibration loads at launch.

These two limitations apply both to the extraction stage (grids 1 and 2) and to the acceleration stage (grids 2 and 3). Considering that the grid gap conventionally used in existing GIE is of the order of 0.5 mm and that this value is the minimum value obtainable keeping reasonable margins over the incurrence of arcing and thermal problems, we can state that this should be kept as an absolute minimum limit also for the acceleration stage gap. Hence, we will assume that for a dual stage ion engine $\lambda = 1$ for values of Γ lower than unity (since as explained above, the value of the gap in the second stage will not be smaller than in the first one) and $\lambda \propto \Gamma$ for values of Γ higher than unity to preserve the maximum electric field.

Using these assumptions together with (3)–(8) and neglecting the value of the accel grid potential in comparison to the screen grid potential the ratio between the thrust density produced by a dual stage ion engine and that produced by a conventional GIE can be expressed as

$$\frac{(T/A)_{DSGIE}}{(T/A)_{GIE}} = \frac{(P/P_{\max})_{DSGIE}}{(P/P_{\max})_{GIE}}\sqrt{1+\Gamma} \quad (9)$$

This article has been accepted for inclusion in a future issue of this journal. Content is final as presented, with the exception of pagination.

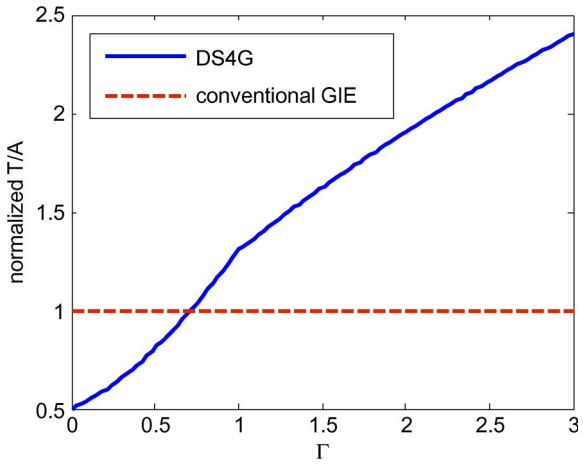

Fig. 5. Dual stage ion engine T/A ratio as a function of Γ normalized with respect to a conventional GIE.

As can be seen from Fig. 5, the dual stage ion engine theoretically offers advantages over a conventional GIE in terms of thrust density only if the potential difference applied in the second stage is 0.6 times the one in the first stage or bigger. Considering the simplified nature of this analysis and taking into consideration the increase in complexity relative to the use of dual stage optics, the dual stage ion engine will probably be a viable and useful option only for values of Γ bigger than unity.

To validate this conclusion, two single hole dual stage ion optics will be numerically investigated using the FFX code developed and extensively validated against experimental measurements at Colorado State University [25], [36], [37]. FFX is a 3-D code that for an hexagonal aperture layout analyzes a rectangular volume containing two quarter sized apertures with symmetry conditions applied on the appropriate sides. The code solves Poisson's equation using a combination of the red-black Gauss-Seidel method with relaxation and the multigrid method. The space charge is introduced calculating the density at each mesh point according to the mesh potential along with the average values of the upstream or downstream ion densities [25]. The plasma sheath shape upstream of the screen grid is calculated self-consistently solving Poisson equation taking into account the electrons barometric law ($n_e = n_{e0} exp[(V_0 - V)/T_{eV}]$) for a fixed electron temperature value. Doubly charged ions, CEX ion production, grid erosion, and sputtered material redeposition are also taken into account.

In the numerical simulations, two values of Γ will be used: 0.6 and 3. These values have been chosen since they correspond, respectively, to a case where the use of a dual stage ion engine should produce small or negligible advantages in terms of thrust density and to a case where a dual stage ion engine should provide a significant thrust density increase.

For both simulations, we will assume an extracted current of 0.3 mA (compatible to the extracted currents of the T6, RIT, and XIPS reported in Table I) and extraction potential drop of about 2000 V (as in most existing GIEs [7]). Given the extraction voltage drop, the selected values of Γ translate into specific impulses of 6250 s ($\Gamma = 0.6$) and 10 000 s ($\Gamma = 3$). In the simulations, we will also avoid the use of a decel (fourth) grid. This is justified by the fact that in a dual stage ion engine, the voltage of the accelerating grid will be of the same order of magnitude as in a conventional GIE (since its function is still to reduce electron backstreaming), hence the entity of CEX erosion that can be expected should be comparable to the one found in conventional GIEs. It can therefore be expected that in this case, as it is for conventional ion engines, the increase in complexity given by the presence of an extra grid will outweigh the benefits deriving from the reduction of CEX erosion on the downstream end of the accelerating grid. From now on, to avoid ambiguity, we will introduce the term DS3G to refer to three gridded dual stage ion engine to distinguish from the DS4G thruster tested at ESTEC [14], [21].

TABLE III
ION OPTICS GEOMETRY

	Aperture radius [mm]	Thickness	Voltage [V]	
			Isp = 6,000 s	Isp = 10,000 s
1st grid	1	0.4 mm	3200	8120
2nd grid	0.8	4x the 1st grid	1200	6120
3rd grid	0.8	4x the 1st grid	-250	-250

For both specific impulse levels under examination, we will use the same grid geometry except for the second stage grid gap. The geometrical parameters have been chosen based on the selected extraction voltage drop and extracted current and on the values commonly used in conventional GIEs [7]. The DS3G screen grid will have apertures of 1-mm radius, whereas the extraction grid apertures will be about 0.8 mm to retain the nonionized propellant and to focus the beam. The accelerating grid will be taken to be identical to the extraction grid. The extraction and acceleration grid thickness will be four times that of the screen grid, the first stage gap will be about 0.5 mm, and the second stage gap has been selected with the aid of the model developed by Holmes and Thompson [38] to minimize the ion beam divergence avoiding at the same time direct ion impingement and arcing between the grids. The overall grid geometry is reported in Table III.

A. Conventional GIE

There are two possible choices regarding the design of the conventional GIE to be compared to the DS3G. It is possible to use a GIE that works at the same Isp level as the DS3G or a GIE that works with the same extraction stage and extracted current.

Both comparisons are valid and provide useful insights into the possible improvements (and/or drawbacks) that the use of two stages produces. However, a DS3G and a GIE producing the same Isp will have extraction stages that are significantly different. This means that the results obtained will be strongly dependent on the level of optimization of the two individual thrusters, hence more difficult to judge impartially.

Comparing instead the performance of a DS3G to those of a conventional GIE having the same extraction characteristics (voltage drop, geometry, and extracted current), the design and optimization of the extraction stage will be common to the two thrusters, hence providing, at this stage, a more solid and reliable comparison since any potential weakness in the GIE design

This article has been accepted for inclusion in a future issue of this journal. Content is final as presented, with the exception of pagination.

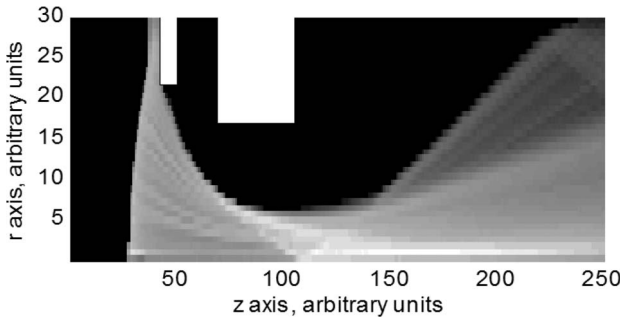

Fig. 6. Beam ion density, conventional GIE, $Isp = 4,600$ s. Arbitrary units.

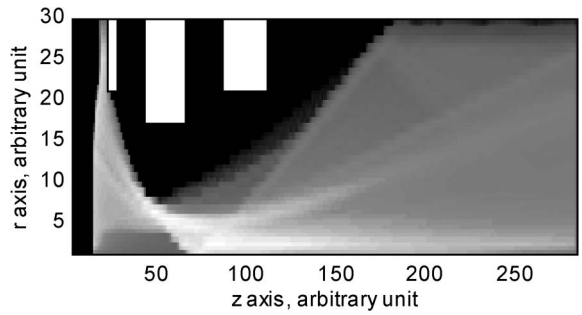

Fig. 7. Beam ion density, $Isp = 10,000$ s. Arbitrary units.

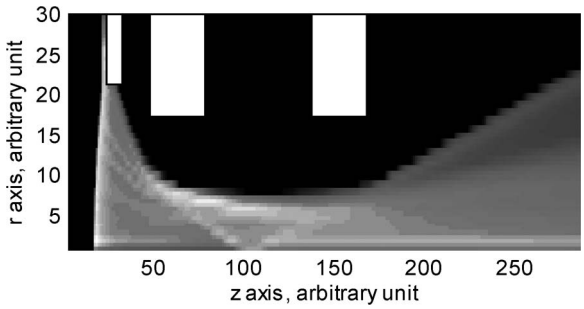

Fig. 8. Beam ion density, $Isp = 6,250$ s. Arbitrary units.

will be "transferred" to the DS3G design. Moreover, such a comparison adds another insight to the possible application of the DS3G since it shows what might be achieved by taking an existing conventional thruster (T5, T6, NSTAR, XIPS, etc.) and adding an extra grid to it to increase its Isp and thrust density.

The conventional ion engine to be compared with the DS3G will have the first two grids equal to the DS3G ones reported in Table II with applied voltages of 1750 V and -250 V, hence having the same extraction potential difference as the DS3G. This GIE has been simulated at a beamlet current level of 0.3 mA.

The ion optics was able to successfully extract 0.3 mA without any direct impingement as it can be seen in Fig. 6. The ion beam divergence was about 10° and the specific impulse about 4600 s.

B. *First Case:* $\Gamma = 0.6$, $Isp = 6,250$

In this case, the value of Γ is about 0.6, hence according to what has been derived above, it should represent the lower limit of application of a dual stage ion engine. In this case, the analytical model [38] produces a very small second grid gap (of the order of 0.1 mm) to try to balance the reduced value of the voltage drop in the second stage. Since the calculated grid spacing is too small, an iterative numerical design was carried out to obtain the smallest possible divergence and erosion rates. The value of the second stage spacing that produces the lowest jet divergence was found to be about 1 mm, but the accelerating grid hole had to be increased to the size of the screen grid one to avoid direct ion impingement. The extracted current (and consequently the P/P_{max} ratio) had to be decreased by about 20% to compensate for the presence of the divergent electrostatic lens correspondent to the second grid.

The focusing of the jet has been examined obtaining a divergence angle of about 10°. For the specific impulse level under consideration, the use of a DS3G will produce a small increase in the T/A ratio with respect to a conventional GIE since the 20% decrease in perveance counterbalances the 34% increase in specific impulse in comparison to the one produced by the conventional GIE. This is in agreement with what has been analytically derived previously showing that a Γ value of 0.6 produces a T/A increase of only 14% that is most probably not enough to justify the increased system complexity and hence can be considered as the absolute lower limit of applicability of dual stage ion optics for ion engines.

C. *Second Case:* $\Gamma = 3$, $Isp = 10,000$

In this case, the model [38] suggests a second stage grid spacing of 1.5 mm which the numerical investigation showed to provide good performance.

As expected, the jet focusing in this case is better than for the 6250 s case showing a divergence of about 3° as can also be seen comparing the ion beam density plot in Fig. 7 to the ones in Figs. 6 and 8. The gridlet system is also able to extract 0.3 mA of current providing at the same time a specific impulse of 10 000 s hence producing roughly twice the thrust density of a conventional GIE operating with a similar extraction stage (since the Isp is about twice and the extracted beamlet current is the same) in agreement with what is shown in Fig. 5.

For what concerns the limit of applicability of a dual stage ion engine, it can be then concluded that the numerical simulations confirmed the analytical predictions, identifying $\Gamma = 0.6$ as the lowest potential ratio value for which a dual stage provides performance improvement in comparison to a conventional GIE. Assuming an extraction potential difference of 2000 V, this lower limit translates into a specific impulse of 6250 s.

VI. Dual Stage Ion Engine Lifetime Simulation

The concerns regarding a DS3G lifetime can be understood by looking at the main lifetime limiting mechanism in GIEs. In gridded ion engines to optimize the overall thruster efficiency, the fraction of propellant that gets ionized is about 70–90% since above this value, the ionization cost in terms of eV needed per ion drastically increases [7]. While the ionized propellant gets accelerated by the electrostatic fields present in the ion optics, the remaining nonionized propellant will drift from the discharge chamber toward the ion optics and finally exit the thruster. Some of the beam ions will undergo CEX collision

This article has been accepted for inclusion in a future issue of this journal. Content is final as presented, with the exception of pagination.

with this nonionized propellant. The CEX ions so produced might then impact on the grids with an energy proportional to the potential of the position where they have been created and the grid voltage.

It is then clear that the higher the potential differences used inside the ion optics, the higher the energy that CEX ions could gain. Even though an increase in the potential difference might improve the jet focusing reducing the amount of ions reaching the grids, the possibility of CEX ions gaining high energy still causes concerns regarding lifetime since the higher the energy of the impinging ions, the higher erosion rate of the grids produced by their impact. Erosion of the grids is the main life limiting mechanism in GIE since it tends to thin the grid thickness (up to the point were a grid undergoes mechanical failure) and to increase the grid aperture size. The increase in accel grid aperture tends to increase the voltage on the hole centerline (since the accel grid voltage is negative and since the bigger the hole the higher the distance to the centerline and the weaker the effect applied voltage) up to the point where the value of the centerline potential is high enough to allow electron backstreaming causing the failure of the thruster) [7].

To verify the effect that the application of dual stage ion optics has on GIE lifetime, a 20-cm dual stage ion optics system able to provide a specific impulse of 10 000 s and a thrust of 0.4 N (in compliance of the requirements reported in Table II) will be taken into account. In particular, in this paper, we will report the results relative to the simulation of the centerline aperture of such system, whereas a more in detail analysis of the whole grids will be the subject of further publications. Since the simulation of the 10 000 s case carried out before provided good results, the DS3G extraction potential drop, grid thickness, apertures diameter, and second stage spacing will be taken to be equal to those presented in Table III for the 10 000 s case. The result obtained from the DS3G simulation will be compared to those obtained from an "equivalent" typical GIE (from now on called TypGIE) having its two grids identical to the first two grids of the DS3G, the same grids potential difference as the first two DS3G grids, the same accel grid potential and working with the same extracted current.

The aim of the simulation will be to evaluate the thruster lifetime and to compare it to the TypGIE one, to the requirements of the HiPER missions and to those of past missions.

We will first present the evolution of the grids shape during lifetime, and then from this, we will determine the operational lifetime of the DS3G and TypGIE.

A. Grid Shape Evolution

In Figs. 9 and 10, the evolution of the radius and thickness of the accel and extraction grids of the DS3G and of the accel grid of the TypGIE are reported in terms of the average aperture radius and grid thickness. The data reported in the figures refer to the aperture relative to the center of the grids. This choice is justified by the fact that the plasma density inside the discharge chamber is maximum on the grid centerline, hence the extracted beamlet current has the highest value there, and consequently also the CEX ions fluxes and hence the erosion rates are maximum on the grid centerline.

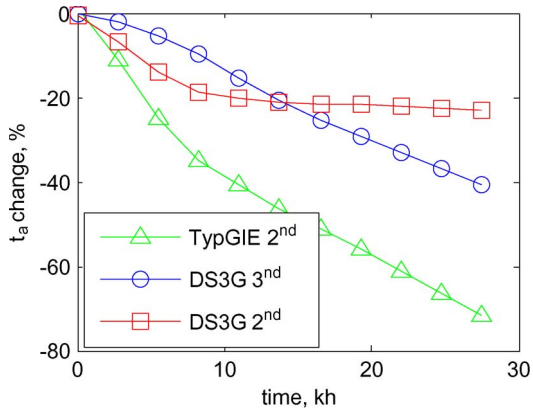

Fig. 9. Change of the mean grid thickness with time for the DS3G and the TypGIE.

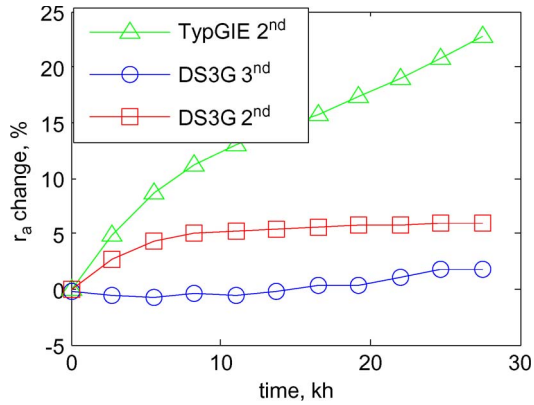

Fig. 10. Change of the mean grid radius with time for the DS3G and the TypGIE.

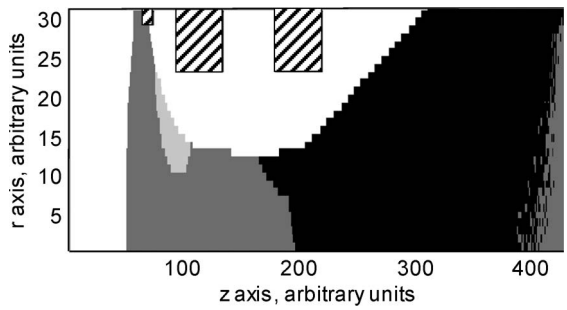

Fig. 11. DS3G CEX ions impingement map.

As it can be seen from Figs. 9 and 10, the accel grid of the TypGIE experience both a marked reduction in thickness and a marked increase in the aperture radius, whereas the accel grid of the DS3G experiences only a reduction in thickness and the extraction grid of the DS3G only an increase in aperture radius.

This difference can be explained looking at the areas of production of CEX ions for the TypGIE and the DS3G shown in Figs. 11 and 12.

In Figs. 11 and 12, the different colors of the different areas indicate where the CEX ions that are produced there will ultimately impact. The CEX produced in the light gray area will impact on the second grid, the ones in the black area on the third one (for the DS3G), whereas the one produced in the dark grey areas will be successfully accelerated by the ion

This article has been accepted for inclusion in a future issue of this journal. Content is final as presented, with the exception of pagination.

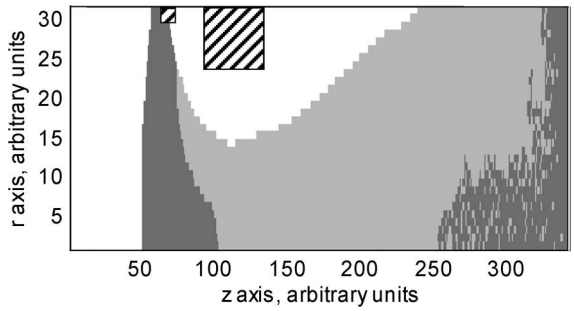

Fig. 12. TypGIE CEX ion impingement map.

optics without impacting on any of the grids. As it can be seen, the area that produces CEX ions that will impact on the accel grid of the TypGIE is "split" in two by the presence of an extra grid in the DS3G. In particular, in a conventional GIE, the CEX ions produced in between the first two grids and the ones produced downstream will both impact on the accel grid producing both a reduction in the grid thickness (mainly due to the ions produced downstream) and an increase of the grid aperture (mainly due to the CEX ions produced in between the first two grids). In a DS3G instead, the presence of an extra grid changes this scenario in such a way that the ions produced in between the first two grids do not impact on the accel grid, hence not producing an increase in the accel grid aperture radius as can be seen in Fig. 10. These ions will instead impact on the DS3G second grid causing its aperture radius to increase with less severe consequences. It must also be noted that the CEX ions produced in between the second and third grid of the DS3G where the highest potential difference is applied (6 kV in this case) get successfully accelerated downstream, hence not producing any damage to the ion optics.

As it can be seen from this first analysis, the consequences of the CEX ions erosion are mitigated on the DS3G due to the presence of an extra grid. This will most probably result in an increased DS3G lifetime as it will be assessed in the next section.

B. Lifetime Prediction

The lifetime of the DS3G and of the TypGIE will be evaluated using two different criteria: the first one based on the thickness reduction of the grids and the second one relative to the change in the minimum centerline potential at the accel grid and to the occurrence of electron backstreaming.

As it has been shown above, the grid that experiences the most severe thinning due to the CEX ions erosion is the accel grid. Making the assumption that the accel grid will fail when its thickness is reduced to zero, the lifetime of the two thrusters can be extrapolated from the data in Fig. 9. The lifetime values so obtained are about 55 000 h for the DS3G and 32 000 h for the TypGIE. It must be noted that these values are best-case lifetime expectations since the grids will actually fail before the grid thickness reaches zero. Nevertheless, the relative importance of this lifetime predictions is still valid showing how the DS3G lasts significantly longer than the TypGIE due to the presence of an extra grid that "splits" in two the CEX fluxes separating the effects relative to the CEX ions produced

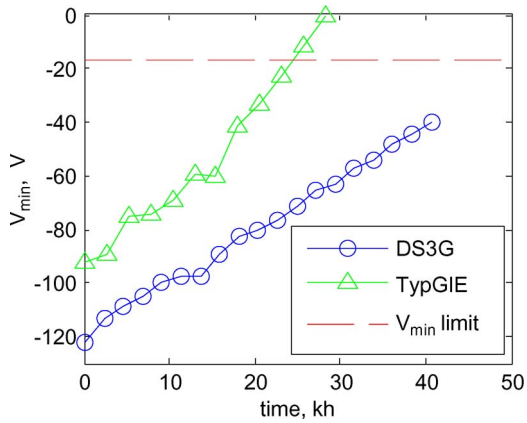

Fig. 13. Trend of the minimum centerline potential with time for the DS3G and the TypGIE at the grid centerline.

in between the grids and of those produced in the downstream plasma.

To obtain a more precise lifetime estimate, the second criterion reported above will be used. In Fig. 13, the trend of the minimum centerline potential is shown.

The minimum centerline potential tends to increase during the lifetime of the thruster due to the accel grid aperture radius increase caused by CEX erosion. When this value exceeds a threshold, electrons will start to backstream into the thruster from the downstream plasma causing high power losses and defocusing the beam leading to the failure of the thruster. The threshold value of the minimum centerline potential can be calculated assuming a Maxwellian distribution of the downstream plasma electrons, fixing a maximum tolerable electron backstreaming current and a value of the downstream electron temperature [39]. Using the values commonly found in conventional GIE of 2 eV for the beam plasma electron temperature and of 0.1% for the ratio between the limiting backstreaming current and the beam current [39], the threshold value of the minimum centerline potential can be calculated to be -17 V.

As it can be seen in Fig. 13, the value of V_{min} is constantly higher for the TypGIE than for the DS3G hence resulting in a longer DS3G lifetime. This can be explained analyzing the influence that the grid geometry and the thruster operating conditions have on the minimum centerline potential. According to [39]V_{min} can be expressed as the sum of the accel grid potential, and of a space charge potential drop and a geometrical voltage drop

$$V_{\min} = V_a + \Delta V_{sc} + \Delta V_{geom} \tag{10}$$

where ΔV_{sc} and ΔV_{geom} are, respectively, the space charge and the geometrical contribution that can be expressed as [39]

$$\Delta V_{sc} = \frac{I_{beam}}{2\pi\varepsilon_0}\frac{1}{v_i}\left[\frac{1}{2} - \ln\left(\frac{r_b}{r_a}\right)\right] \tag{11}$$

$$\Delta V_{geom} = \frac{|V_b - V_a| r_a}{\pi l_e}\left[1 - \frac{t_a}{r_a} tan^{-1}\left(\frac{r_a}{t_a}\right)\right] exp\left(-\frac{t_a}{r_a}\right) \tag{12}$$

where r_b and v_i are the beamlet radius and the ion velocity at the accel grid, V_b is the ion beam voltage and V_a, r_a and t_a stand for the accel grid voltage, aperture radius, and thickness. Given

This article has been accepted for inclusion in a future issue of this journal. Content is final as presented, with the exception of pagination.

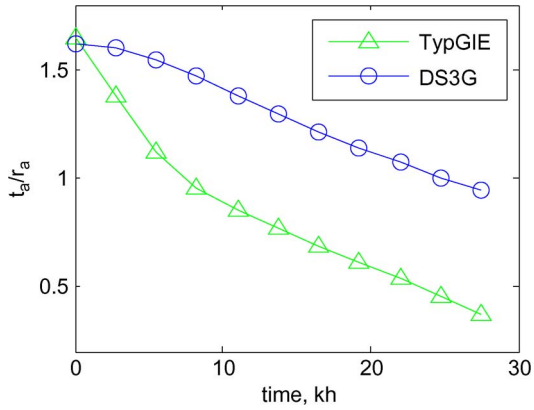

Fig. 14. Change of the t_a/r_a ratio with time for the DS3G and the TypGIE.

the higher Isp (and hence higher ion velocity) of the DS3G, its value of ΔV_{sc} is about half the one of the TypGIE explaining why the DS3G shows a lower value of V_{min} at the beginning of life. From Fig. 13, it is clear how the value of the minimum centerline potential increases more quickly for the TypGIE than for the DS3G; this is due to the different evolution of the accel grid thickness and radius for the TypGIE and the DS3G (Figs. 9 and 10) and in particular, according to (12), to a different trend of the t_a/r_a ratio for the two thrusters (Fig. 14).

Looking at Fig. 14, it can be seen how for the TypGIE the thickness to aperture radius ratio decreases more during the lifetime than for the DS3G. Noting that, as reported in (12), ΔV_{geom} increases as t_a/r_a decreases, the trends in Fig. 13 can be explained.

Using the data reported in Fig. 13, the lifetime of the two thrusters can be extrapolated obtaining a value of about 25 000 h for the TypGIE and of about 50 000 h for the DS3G. As expected, these values are lower than the ones obtained from the extrapolation of the thickness trend but still show how the lifetime of the DS3G is significantly longer than the TypGIE one.

The lifetime values so obtained can be compared to those required by previous missions where GIEs were employed and to those required by the HiPER missions. In particular, the lifetime obtained for the TypGIE is sufficient to achieve the requirements of the Deep Space 1 and GOCE mission (about 20 000 h [12], [40]) and of the Bepi Colombo mission (about 17 000 h [13]) but not enough if compared to the requirements specified in Table II. On the contrary, the DS3G shows lifetime in excess of those required by past missions and of those required by the HiPER project (28 000 h for the EML1 infrastructure and 45–48 000 h for Mars Infrastructure and NEP mission to Saturn).

VII. Conclusion

In this paper, the limits of conventional gridded ion engines have been explained and their possible application to future high power high specific impulse missions analyzed. It has been concluded that there is a need to increase the thrust density that these thrusters can produce. This increase can be achieved using thrusters with dual stage ion optics. New results are presented for the first time in the open literature on the limits of applicability of this type of ion optics to space propulsion and its effects on the thruster lifetime. The limits of applicability of dual stage ion optics to gridded ion engines have been studied both analytically and numerically with the numerical result confirming the analytical predictions. In particular, it has been found that dual stage ion optics is beneficial in terms of thrust density increase for ion propulsion if the ratio between the potential drop in the second stage to the one on the first stage (Γ) is bigger than 0.6. In particular, if an extraction voltage drop of 2000 V is assumed specific impulses in excess of 6250 s must be used.

Subsequently, the lifetime of a dual stage ion engine has been numerically analyzed and compared to the one produced by a "typical" gridded ion engine having equivalent geometry and operational conditions (same geometry of the first two grids and same extraction voltage and extracted current). The dual stage ion engine has been found to provide longer lifetime than the conventional one due to the fact that using three grids, the CEX production regions are split in two, lowering the erosion rates of the accel grid. The computed lifetime has been found to be compliant with the HiPER requirements and with those of past missions where GIEs have been employed. Moreover, the simulated dual stage ion engine gridlet was able to produce a thrust density of 12.7 N/m^2 proving a significant increase over conventional GIEs (Table II) and in particular in comparison to GIEs working at similar Isp level.

The goal of such simulation was not to determine if a dual stage ion engine is better than any "conventional" gridded ion engine but to assess the effect that the use of dual stage ion optics have on a gridded ion engine lifetime.

In particular, given the assumption of the DS3G and GIE having extraction stages that are equivalent in terms of geometry, extracted current, and extraction potential, and given the reported results, it can be stated that the conversion of an existing GIE into a dual stage ion engine with the aim of increasing its specific impulse, thrust density, and processed power will not cause any penalty in the engine lifetime.

Moreover, a careful design of the second stage can improve the thruster lifetime splitting the CEX flux originally impacting on the GIE accel grid between the DS3G second and third grid. It must also be noted that the better the lifetime of the GIE, the better the one of the DS3G obtained adding a grid to it since, according to the assumption made, the two thrusters have the same extraction stage.

In conclusion, the use of dual stage ion engines, due to their capability of providing high Isp, high thrust density, and long lifetime, appears to be very promising for future high power, high Isp missions. Future work will consist in performing numerical parametric study to analyze in depth the DS3G ion optics capabilities and, possibly, in building and testing a thruster prototype.

Acknowledgment

The authors would like to thank Dr. C. Farnell and Prof. J. Williams from Colorado State University for the help and useful discussions regarding the numerical simulations presented in this paper.

This article has been accepted for inclusion in a future issue of this journal. Content is final as presented, with the exception of pagination.

REFERENCES

[1] C. Garner, M. Rayman, and J. Brophy, "The dawn of Vesta Science," presented at the 32nd International Electric Propulsion Conference, Wiesbaden, Germany, 2011, Paper IEPC-2011-326.

[2] J. Brophy, C. Garner, and S. Mikes, "Dawn ion propulsion system: Initial checkout after launch," *J. Propulsion Power*, vol. 25, no. 6, pp. 1189–1202, 2009.

[3] J. R. Brophy, M. G. Marcucci, G. B. Ganapathi, C. E. Garner, M. D. Henry, B. Nakazono, and D. Noon, "The ion propulsion system for dawn," presented at the 39th AIAA Joint Propulsion Conference, Huntsville, AL, 2003, AIAA-2003-4542.

[4] [Online]. Available: http://nmp.nasa.gov/ds1/

[5] [Online]. Available: http://www.esa.int/esaLP/LPgoce.html

[6] [Online]. Available: http://www.esa.int/esaSC/120391_index_0_m.html

[7] D. M. Goebel and I. Katz, "Fundamentals of electric propulsion: Ion and hall thrusters," in *NASA JPL Space and Technology Series*. New York: Wiley, 2008.

[8] H. R. Kaufmann, "Technology of electron-bombardment ion thrusters," *Adv. Electron. Electron Phys.*, vol. 36, pp. 265–373, 1974.

[9] C. Casaregola, G. Cesaretti, and M. Andrenucci, "HiPER: A roadmap for future space exploration with innovative electric propulsion technologies," presented at the 31st International Electric Propulsion Conference, Ann Arbor, MI, Sep. 20–24, 2009, Paper IEPC-2009-066.

[10] H. Kuninaka, K. Nishiyama, I. Funaki, Tetsuya, Y. Shimizu, and J. Kawaguchi, "Asteroid rendezvous of HAYABUSA explorer using microwave discharge ion engines," presented at the 29th International Electric Propulsion Conference, Kanagawa, Japan, 2005, Paper IEPC-2005-10.

[11] J. Polk, R. Y. Kakuda, D. Brinza, I. Katz, J. R. Anderson, J. R. Brophy, V. K. Rawlin, M. J. Patterson, J. S. Sovey, and J. Hamley, "Demonstration of the NSTAR ion propulsion system on the deep space one mission," presented at the 27th International Electric Propulsion Conference, Pasadena, CA, Oct. 15–19, 2001, Paper IEPC-01-075.

[12] C. Edwards and N. C. Wallace, "The T5 ion propulsion assembly for drag compensation on GOCE," in *Proc. 2nd Int. GOCE User Workshop*, Frascati, Italy, 2004.

[13] N. C. Wallace, "Testing of the Qinetiq T6 thruster in support of the ESA BepiColombo mercury mission for the ESA BepiColombo mission," in *Proc. 4th Int. Spacecraft Propulsion Conf.*, Sardinia, Italy, 2004.

[14] C. Bramanti and D. Fearn, "The design and operation of beam diagnostics for the dual stage 4-grid ion thruster," presented at the 30th International Electric Propulsion Conference, Florence, Italy, Sep. 17–20, 2007, Paper IEPC-2007-050.

[15] J. R. Coupland and E. Thompson, "The production of high current, high quality beams of ions and neutral particles," *Rev. Sci. Instrum.*, vol. 42, no. 7, pp. 1034–1037, Jul. 1971.

[16] J. Kim, W. L. Gardner, and M. M. Menon, "Experimental study of ion beam optics in a two-stage accelerator," *Rev. Sci. Instrum.*, vol. 50, no. 2, pp. 201–206, Feb. 1979.

[17] A. R. Martin, "High power beams for neutral injection heating," *Vacuum*, vol. 34, no. 1/2, pp. 17–24, 2001.

[18] Y. Okumura, S. Matsuda, Y. Mizutani, Y. Ohara, and T. Ohga, "Quasi-dc extraction of 70 keV, 5 A ion beam," *Rev. Sci. Instrum.*, vol. 51, no. 6, pp. 728–734, Jun. 1980.

[19] M. Taniguchi, T. Mizuno, N. Umeda, M. Kashiwagi, K. Watanabe, H. Tobari, A. Kojima, Y. Tanaka, M. Dairaku, M. Hanada, K. Sakamoto, and T. Inoue, "Long pulse H- ion beam acceleration in MeV accelerator," *Rev.Sci.Instrum.*, vol. 81, no. 2, Feb. 2010.

[20] T. Inoue, M. Kashiwagi, M. Taniguchi, M. Dairaku, M. Hanada, K. Watanabe, and K. Sakamoto, "1 MeV, ampere class accelerator R&D for ITER," *Nucl. Fusion*, vol. 46, no. 6, pp. S379–S385, May 2006.

[21] R. Walker, C. Bramanti, O. Sutherland, R. Boswell, C. Charles, D. Fearn, J. Gonzalez Del Amo, P. E. Frigot, and M. Orlandi, "Initial experiments on a dual-stage 4-grid ion thruster for very high specific impulse and power," presented at the 42nd AIAA/ASME/SAE/ASEE Joint Propulsion Conference & Exhibit, Sacramento, CA, 2006, AIAA-2006-4669.

[22] R. Walker, C. Bramanti, O. Sutherland, P. E. Frigot, M. Orlandi, and D. Fearn, "SAFE/DS4G Thruster Test Report #1," ESA ESTEC report ACT-RPT-4100-05-SAFETEST, 2006.

[23] R. Jahn, *Physics of Electric Propulsion*. New York: McGraw-Hill, 1968.

[24] J. R. Pierce, *Theory and Design of Electron Beams*, 2nd ed. New York: Van Nostrand, 1954.

[25] C. C. Farnell, J. D. Williams, and P. J. Wilbur, "NEXT Ion Optics Simulation via ffx," Colorado State Univ., Huntsville, AL, Tech. Rep. NASA/CR-2003-212594, 2003.

[26] E. R. Harrison, "Investigation of the perveances and beam profiles of an aperture disk emission system," *J. Appl. Phys.*, vol. 29, no. 6, pp. 909–913, Jun. 1958.

[27] J. E. Foster, T. Haag, M. Patterson, G. Williams, J. S. Sovey, C. Carpenter, H. Kamhawi, S. Malone, and F. Elliot, "The High Power Electric Propulsion (HiPEP) Ion Thruster," Glenn Res. Center, Cleveland, OH, Tech. Rep. NASA/TM-2004-213194, 2004.

[28] J. Snyder, D. M. Goebel, J. E. Polk, A. C. Schneider, and A. Sengupta, "Results of a 2000-hour wear test of the NEXIS ion engine," presented at the 29th International Electric Propulsion Conference, Pasadena, CA, 2005, Paper IEPC-2005-281.

[29] J. Snyder, J. Anderson, G. Soulas, and J. Van Noord, "Environmental testing of the NEXT PM1R ion engine," presented at the 30th International Electric Propulsion Conference, Florence, Italy, Sep. 17–20, 2007, Paper IEPC-2007-276.

[30] S. Kitamura, Y. Okawa, Y. Hayakawa, H. Yoshida, and K. Miyazaki, "Overview and research status of the JAXA 150-mN ion engine," *Acta Astronaut.*, vol. 61, no. 1–6, pp. 360–366, Jun.–Aug. 2007.

[31] H. Leiter, R. Killinger, R. Kukies, and T. Frohlich, "Extended performance evaluation of EADS ST's 200 mn radio frequency ion thruster," presented at the 39th AIAA Joint Propulsion Conference, Huntsville, AL, 2003, AIAA 2003-5010.

[32] J. Snyder, D. M. Goebel, R. Hofer, J. Polk, N. Wallace, and H. Simpson, "Performance evaluation of the T6 ion engine," presented at the 46th AIAA/ASME/SAE/ASEE Joint Propulsion Conference & Exhibit, Nashville, TN, Jul. 25–28, 2011, AIAA-2010-7114.

[33] C. J. Davisson and C. J. Calbick, "Electron lenses," *Phys. Rev.*, vol. 42, no. 4, p. 580, Nov. 1932.

[34] J. Kim, J. H. Whealton, and G. Schilling, "A study of two-stage ion-beam optics," *J. Appl. Phys.*, vol. 49, no. 2, pp. 517–524, Feb. 1978.

[35] J. R. Coupland, T. S. Green, D. P. Hammond, and A. C. Riviere, "A study of the ion beam intensity and divergence obtained from a single aperture three electrode extraction system," *Rev. Sci. Instrum.*, vol. 44, no. 9, pp. 1258–1270, Sep. 1973.

[36] C. C. Farnell, J. D. Williams, and P. J. Wilbur, "Numerical simulation of ion thruster optics," presented at the 28th International Electric Propulsion Conference, Toulouse, France, 2003, Paper IEPC-03-73.

[37] J. D. Williams, C. C. Farnell, D. A. Laufer, and R. A. Martinez, "HiPEP ion optics system evaluation using gridlets," presented at the 40th AIAA Joint Propulsion Conference, Fort Lauderdale, FL, 2004, AIAA-2004-3814.

[38] A. J. T. Holmes and E. Thompson, "Beam steering in tetrode extraction systems," *Rev. Sci. Instrum.*, vol. 52, no. 2, pp. 172–179, Feb. 1981.

[39] J. D. Williams, D. M. Goebel, and P. J. Wilbur, "39th AIAA Joint Propulsion Conference," presented at the Analytical model of electron backstreaming for ion thrusters, Huntsville, AL, 2003, AIAA 2003-4560.

[40] J. S. Sovey, L. A. Hamley, T. Haag, M. J. Patterson, A. John, E. J. Pencil, T. T. Peterson, L. R. Pinero, J. L. Power, V. K. Rawlin, C. J. Sarmiento, J. R. Anderson, T. A. Bond, G. I. Cardwell, and J. A. Christensen, "Development of an Io Thruster and Power Processor for the New Millenniumàs Deep Space 1 Mission," NASA, Seattle, WA, Tech. rep. NASA-TM-113129, 1997.

Michele Coletti received the B.Sc. degree in aerospace engineering from the University of Rome "La Sapienza," Rome, Italy, in 2003, the M.Sc. degree in astronautics engineering from the "Scuola di Ingegneria Aerospaziale," Univeristy of Rome "La Sapienza," in 2005, and the Ph.D. degree in electric propulsion form the University of Southampton, Southampton, U.K., in 2008 working on hollow cathode lifetime modeling.

He is currently involved in research and development on hollow cathodes, hollow cathodes thrusters, high power gridded ion engines, and micro PPT for cubesat and nanosatellites applications both at the University of Southampton and at Mars Space Ltd, Southampton.

Stephen B. Gabriel, photograph and biography not available at the time of publication.